Proc. Natl. Acad. Sci. USA
Vol. 95, pp. 11257–11262, September 1998
Developmental Biology

Identification and characterization of *LMO4*, an LMO gene with a novel pattern of expression during embryogenesis

(LHX genes/nuclear LIM interactor/cranial neural crest/Schwann cells/somite)

DARYN A. KENNY*, LINDA W. JURATA†, YUMIKO SAGA‡, AND GORDON N. GILL*§

*Department of Medicine and †Biomedical Sciences Graduate Program, University of California at San Diego, La Jolla, CA 92093-0650; and ‡Cellular and Molecular Toxicology, National Institute of Health Science, Kamiyohga, Setagaya-ku, 158 Japan

Communicated by Anthony Rex Hunter, The Salk Institute for Biological Studies, San Diego, CA, July 16, 1998 (received for review June 3, 1998)

ABSTRACT ***LMO4* is a novel member of the LIM-only (LMO) subfamily of LIM domain-containing transcription factors. *LMO1, LMO2*, and *LMO4* have distinct expression patterns in adult tissue, and we demonstrate that nuclear retention of LMO proteins is enhanced by the nuclear LIM interactor (NLI). *In situ* hybridization to early mouse embryos of 8–14.5 days revealed a complex pattern of *LMO4* expression spatially overlapping with *NLI* and *LHX* genes. *LMO4* expression in somite is repressed in mice mutant for the segment polarity gene *Mesp2* and expanded in *Splotch* mutants. During jaw and limb outgrowth, *LMO4* and *LMO2* expression define mesenchyme that is uncommitted to regional fates. Although both *LMO2* and *LMO4* are activated in thymic blast cells, only *LMO4* is expressed in mature T cells. Mesenchymal and thymic blast cell expression patterns of *LMO4* and *LMO2* are consistent with the suggestion that LMO genes inhibit differentiation.**

The LIM domain, an approximately 55-residue, cysteine-rich zinc-binding motif, is present in a variety of proteins including LIM homeobox (LHX) proteins that contain two LIM domains and one homeodomain. *LHX* genes are expressed in many types of neurons and other cell types, and deletion of *LHX g*enes results in the loss of cell fate (1). Mice mutant for *LHX1* have diminished organizer activity that results in lack of head structures anterior to rhombomere 3 (2). In the central nervous system, development of forebrain and pituitary derivatives are defective in mice mutant for *LHX2*, *LHX3*, or *LHX4* (1), while activation of the *LHX* gene *Isl1* is essential for the survival of motor neurons and neighboring interneurons (3).

LMO2 represents a family of nuclear LIM-only (LMO) proteins that lack a DNA-binding homeodomain (4, 5). Unregulated *LMO2* expression induces T cell tumors (6), while deletion blocks hematopoietic development (7, 8). The mechanism of LMO2 activity is thought to be the LIM domain-dependent assembly of transcription complexes and transcription regulation (9).

LIM domains of nuclear proteins bind with high affinity to the widely expressed nuclear LIM interactor (NLI) and with lesser affinity to other transcription factors (10–12). Dimeric NLI supports assembly of heteromeric complexes of LIM proteins (13), and CHIP, the *Drosophila* ortholog of NLI, mediates enhancer–promoter interactions of the cut and ultrabithorax genes, presumably by complex formation with transcription factors (14).

To identify novel LIM domain transcription factors, we screened two mouse embryonic expression libraries by using the LIM interaction domain (LID) of NLI. We report the isolation and characterization of *LMO4*, a novel LIM-only gene, which is highly expressed in the T lymphocyte lineage, cranial neural crest cells, somite, dorsal limb bud mesenchyme, motor neurons, and Schwann cell progenitors. Somitic expression of *LMO4* is repressed in mice mutant for the segment polarity gene *Mesp2. LMO4* and *LMO2* expression in the jaw, limb, and thymus defines cells that are uncommitted to cell fates. Interaction with NLI mediates the nuclear retention of LMO proteins that lack a nuclear localization sequence.

MATERIALS AND METHODS

Expression Library Screening and Sequence Analysis. A cDNA fragment encoding the LID (NLI amino acids 300–338) was amplified by PCR with Pfu polymerase (Stratagene) and subcloned into pGEX-2TK (Pharmacia). The GST-TK-LID fusion protein was purified by standard procedures, labeled with [γ-^{32}P]ATP, and used to screen mouse E12 and E16 λ-ExLox expression libraries (Novagen) as described previously (10). Positive clones were purified and the cDNAs were subcloned from phage DNA. Sequence information from the 5′ end of each clone was analyzed by BLAST (http://www.ncbi.nlm.nih.gov/BLAST/). Phylogenetic sequence analysis was performed by using the PILEUP, DISTANCES, and GROWTREE programs of the GCG software package.

RNA Purification and PCR Analysis. Total RNA from flow cytometry-sorted thymocytes was isolated by using Rneasy spin columns (Qiagen). For reverse transcription–PCR, 200 ng total RNA from each thymic subset was converted to cDNA by using the Superscript II kit (GIBCO/BRL), and resulting samples were subjected to 35 cycles of the PCR by using Boehringer *Taq* polymerase and 7.5 pmol of each primer. Amplified material was resolved by agarose gel electrophoresis and visualized with ethidium bromide.

***In Situ* Hybridization and Immunohistochemistry.** *In situ* hybridization of [^{35}S]UTP- or digoxygenin-labeled probes to tissue sections was performed as described previously (15–17). Linear templates for probe synthesis were generated as follows: LMO4pBSIIKS+/*Acc*I for 750-bp probe, LMO2pGEM3z/*Eco*RI for 1.1-kb probe; LHX3pcDNA3/*Eco*RI; SOX10pZL1/*Ava*I for 1-kb probe; Pax3pBSIIKS+/*Hin*dIII for 0.8-kb probe; Ptx1pcDNA3/*Eco*RI for 0.95-kb probe. For immunohistochemistry, HB9 antibody was diluted to 1:8,000. HRP anti-rabbit (The

Abbreviations: LHX, LIM homeobox; LMO, LIM-only family of nuclear LIM proteins; NLI, nuclear LIM interactor (also named Ldb1, LIM domain-binding protein; CLIM, cofactor of LIM homeodomain proteins); LID, LIM interaction domain of NLI; AER, apical ectodermal ridge; ZPA, zone of polarizing activity; DRG, dorsal root ganglia.

Data deposition: The sequence reported in this paper has been deposited in the GenBank database [accession no. AF074600 (mouse *LMO4*)].

§To whom reprint requests should be addressed at: University of California at San Diego, 9500 Gilman Drive, La Jolla, CA 92093-0650. e-mail: ggill@ucsd.edu.

The publication costs of this article were defrayed in part by page charge payment. This article must therefore be hereby marked "*advertisement*" in accordance with 18 U.S.C. §1734 solely to indicate this fact.

Jackson Laboratory) secondary antibody was used at 1:400, and peroxidase reactions were done according to the manufacturer's protocol. Other antibodies included mouse anti-hemagglutinin (HA) epitope antibody (HA.11), 1:1,000; rabbit anti-NLI antibody (4508), 1:500; HiFITC anti-mouse (Antibodies, Inc.), 1:300; and Cy3 anti-rabbit (The Jackson Laboratory), 1:300.

RESULTS

Identification of a Novel LIM-Only Gene, LMO4. To isolate novel LIM domain-containing transcription factors, mouse embryonic day 12 (E12) and 16 (E16) lambda expression libraries were screened with the LID of NLI. Of 2.6×10^6 E12 phage clones screened, two Isl1, two LH-2a (LHX2), one LHX5, and five LMO2 cDNAs were isolated. In addition, 13 phage clones contained cDNAs encoding an as yet uncharacterized LMO protein, which we designated LMO4. The eight positive clones out of 1.3×10^6 E16 phages screened included two LMO1 cDNAs and six LMO4 cDNAs.

Conceptual translation of the LMO4 cDNA indicated a single ORF encoding a 165-aa protein of approximately 19 kDa, similar in size to the known mammalian LMO proteins, LMO1, LMO2, and LMO3 (18). The human homolog of LMO4 has been deposited in GenBank (accession no. U24576). Sequence comparison of the LMO4 protein to known mammalian and *Drosophila* LMO proteins indicated that LMO4 is the most distantly related of the LMO family members, with only about 50% amino acid identity within the LIM domains to other LMO proteins (Fig. 1 *A* and *B*). In contrast, the LIM domains of LMO1 and the nearly identical LMO3 show 78% identity to the only known *Drosophila* LMO protein, dLMO (19), and likely represent the vertebrate orthologs of dLMO.

Because LMO proteins display significant sequence homology and similar functional characteristics to the LHX proteins, e.g., nuclear localization, high-affinity interaction with NLI, and assembly into transcription complexes, it is likely that these two subfamilies arose from a gene-duplication event at some point in evolution. Sequence comparison of LIM domains indicates that the LMO proteins are more closely related to the LHX proteins L3 and the LH-2 subgroup (which includes vertebrate LH-2a, LH-2b, the *Drosophila* protein apterous, and the *Caenorhabditis elegans* ttx-3) than to any other LHX protein, suggesting that the LMO genes arose from an ancestral LH-2 or L3-like gene (Fig. 1*C*).

***In Vitro* and *in Vivo* Interaction of LMO4 with NLI.** LMO4:NLI interactions were investigated *in vitro* and *in vivo*. Glutathione *S*-transferase (GST) fusion assays in which GST-NLI fusion proteins were incubated with [^{35}S]methionine-labeled LMO4 indicated that LMO4 and NLI associate with high affinity (Fig. 2*A*), and that the LID of NLI was required and sufficient for interaction with LMO4. When coexpressed with exogenous NLI in embryonic kidney 293 cells, LMO1, LMO2, and LMO4, but not the cytoskeletal-associated LIM protein CRP, coprecipitated efficiently with anti-NLI antibodies (Fig. 2*B*).

The small size of LMO proteins suggests that they should be capable of freely traveling in and out of the nucleus; however, the lack of a nuclear localization signal (NLS) sequence in the LIM-only transcription factors suggests that they lack an intrinsic mechanism for nuclear retention. It is therefore unclear how LMO proteins are localized predominately in the nucleus (7). Using an anti-HA epitope antibody, immunocytochemistry of 293 cells transfected with HA-tagged LMO2 or LMO4 showed distribution in both the nucleus and cytoplasm (Fig. 2*C*, *a* and *e*). However, upon cotransfection of the LMO cDNAs with NLI, anti-HA and anti-NLI immunocytochemistry revealed a predominantly nuclear localization (Fig. 2*C*, *b–d*, *f*). NLI contains at least two NLS sequences and is a nuclear protein (10). Since cotransfection of NLI with LMO cDNAs promoted nuclear retention of LMO proteins, the partial nuclear distribution of LMO2 and LMO4 in cells not transfected with NLI is likely a result of endogenous NLI (Fig. 2*C*, *d*). These results indicate that one function of NLI in cells is to maintain the nuclear localization of LMO proteins.

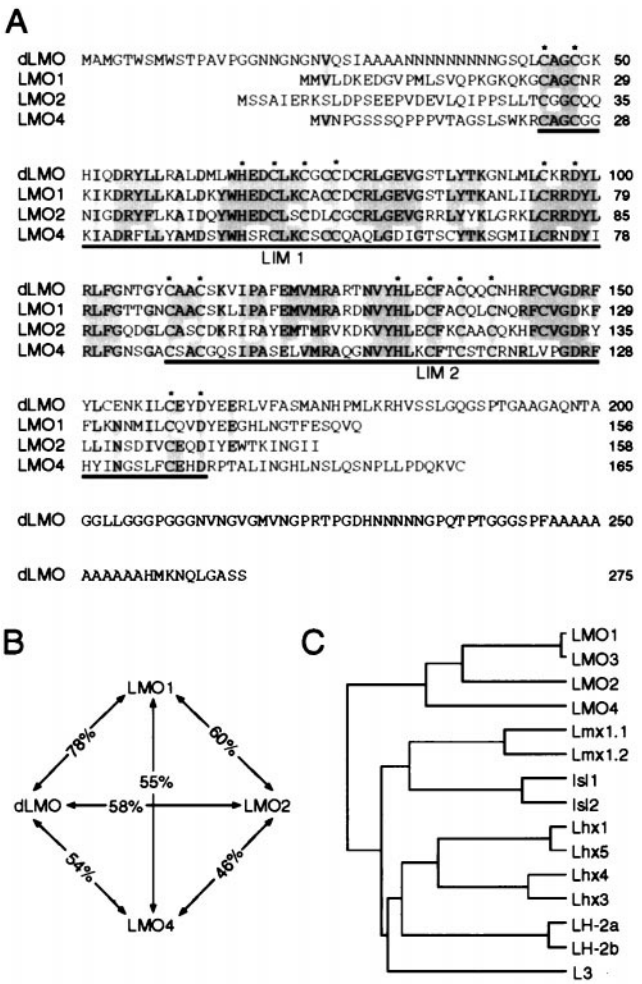

FIG. 1. Sequence analysis of LMO4. (*A*) Sequence alignment of mouse LMO4 with LMO1 and LMO2, and *Drosophila* LMO. Shading shows conservation of amino acids, and asterisks indicate the zinc-coordinating residues of each LIM domain. (*B*) Diagram illustrating relative amino acid sequence identity between the LIM domains of LMO family members. (*C*) Dendrogram showing genealogical relationships between the LIM domains of LMO and LHX proteins. Comparisons were made using only the LIM domain sequences and inter-LIM region of the rodent representative of each gene, except for LH-2a and LH-2b, which were from chick.

Differential *LMO* mRNA Expression in Adult Mouse Tissues. To compare the tissue distribution of *LMO4* gene expression with other LMO genes, Northern blots of poly(A)$^+$ RNA isolated from E12 mouse embryos and various adult mouse tissues were compared. While low levels of *LMO1* expression could be detected only in the E12 embryo, eye, brain, and skeletal muscle, *LMO2* expression was highest in the E12 embryo, spleen, and lung as noted previously (5, 18, 20) (Fig. 3*A*). The signals in the lung and spleen lanes of the *LMO1* blot are the result of residual hybridization of the *LMO2* probe. Low-level expression of *LMO2* was detectable in the thymus as noted previously (20). In contrast to the relatively restricted pattern of expression of *LMO1* and *LMO2, LMO4* mRNA was more widely expressed, with highest levels in the eye, brain, kidney, and, intriguingly, the thymus. The mRNA expression of *LMO* genes in adult tissues is overlapping, but clearly distinct.

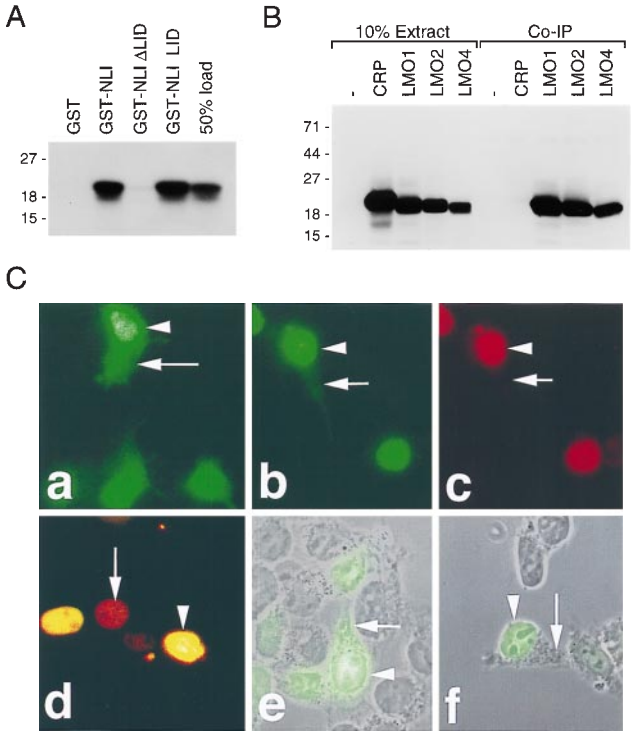

FIG. 2. Association of LMO proteins with NLI *in vitro* and *in vivo*. (*A*) GST-NLI fusions were incubated with *in vitro*-translated, [^{35}S]methionine-labeled LMO4, and 50% of the *in vitro*-translated material used in the binding reaction was loaded separately for estimation of binding affinity. Interaction was visualized by SDS/PAGE and fluorography. (*B*) *In vivo* association of LMO proteins with NLI. Anti-NLI immunoprecipitation and anti-HA epitope immunoblotting of whole-cell extracts from cotransfected 293 cells. Ten percent of the extracts was loaded separately to show relative expression. (*C*) Nuclear retention of LMO proteins depends on NLI. Immunohistochemistry using an anti-HA epitope antibody (Babco, Richmond, CA) showed diffuse localization of HA-tagged LMO2 (*a*) and LMO4 (*e*) in transiently transfected 293 cells. Cotransfection of untagged NLI with LMOs resulted in nuclear retention of LMO2 (*b*) and LMO4 (*d* and *f*). NLI was localized to the nucleus (*c* and *d*). (*d*) Merging of NLI and HA-LMO4 staining shows codistribution in cell nuclei (arrowhead) and endogenous expression of NLI (arrow). For *e* and *f*, transmitted light images of differential interference contrast optics were captured in registration with the fluorescent signals.

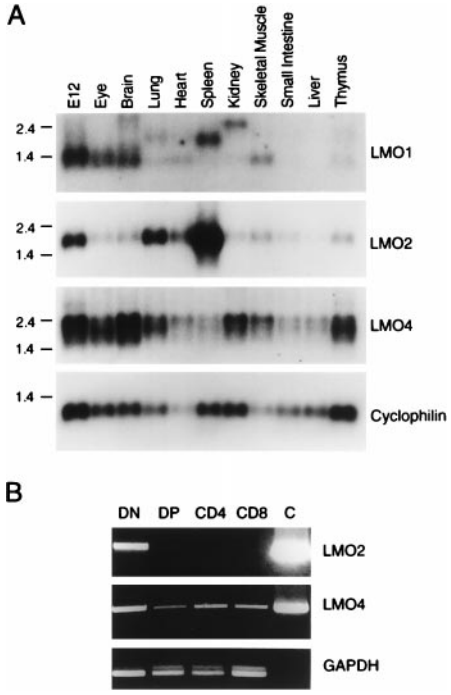

FIG. 3. (*A*) Northern analysis of various adult mouse tissues and the E12 embryo shows combinatorial and complementary patterns of expression of *LMO* genes. (*B*) Reverse transcription–PCR analysis of thymic sublineages. Glyceraldehyde-3-phosphate dehydrogenase (GAPDH) estimates relative quantities of cDNAs in each lane. C is a control PCR product from 0.1 μg of the appropriate template cDNA. DN, double-negative ($CD3^-CD4^-CD8^-$); DP, double-positive ($CD4^+CD8^+$).

Because unregulated expression of *LMO1* (21) and *LMO2* (6) in T cells results in leukemogenesis, we examined the expression of *LMO4* in adult thymus tissue at a cellular level. *In situ* hybridization showed widespread expression of *LMO4* throughout the thymus, consistent with expression in the lymphoid lineage (not shown). To identify the types of lymphoid cells that express *LMO4* and *LMO2*, we isolated the four major thymic subsets: immature blast cells (DN), negative for CD3, CD4, and CD8; $CD4^+CD8^+$ double-positive cells (DP); and single-positive (SP) mature $CD4^+$ or $CD8^+$ cells. The DN cells are predominantly immature T cells, but may contain trace amounts of non-T cells of the lymphoid lineage. As shown in Fig. 3*B*, *LMO4* was expressed in all of the four major thymic subsets, while *LMO2* expression was restricted to the immature blast cells. Therefore, *LMO4* and *LMO2* are coexpressed in proliferating blast cells, but differentially regulated in double-positive and single-positive subsets.

***LMO4* Expression During Somitogenesis.** To analyze the temporal and spatial patterns of *LMO4* expression in the embryo, an *LMO4* probe was used in *in situ* hybridization experiments in whole mount and on sections. In the 16 somite-stage embryo (E9.0), *LMO4* expression was distributed rostrally in migratory cranial crest within the branchial arches, and caudally in dorsal paraxial mesoderm (Fig. 4*A*). In paraxial mesoderm, expression was initially restricted dorsally (Fig. 4*A*, a). The metameric pattern of expression seen in the presomitic mesoderm was maintained in the somite, as *LMO4* was restricted to the rostral portion of each somite (Fig. 4*A*, b and c). *LMO4* expression persisted in paraxial mesoderm at E9.5, with highest levels observed in the rostral portion of the first few newly formed somites (Fig. 4*B*). At anterior axial levels, *LMO4* expression was restricted to cells adjacent to the neural tube (Fig. 4*D*). Thus, *LMO4* is activated in cranial neural crest cells and dorsal paraxial mesoderm.

We compared the pattern of expression of *LMO4* with that of *Pax3,* a paired-type Hox gene known to be expressed in neural crest and the dermomyotome (22, 23). Unlike *LMO4*, which is restricted to the rostral portion of newly formed somites, and restricted medially in mature somites (Fig. 4*B*), *Pax3* expression persisted throughout the dermomyotome in mature somites (Fig. 4*C*). The observation that *LMO4* and *Pax3* are coexpressed initially raised the possibility that *LMO4* might be regulated by Pax3. In *Splotch* mutants, which lack functional Pax3, *LMO4* was activated normally in unsegmented dorsal mesoderm and in migratory cranial crest (Fig. 4*F*). However, the domain of *LMO4* expression in mature somites persisted laterally in *Splotch* embryos (Fig. 4*F*), raising the possibility that Pax3 may normally restrict expression of *LMO4*.

LMO4 activation in *Mesp2* mutants was examined to discern whether *LMO4* expression is linked to somite segment polarity or differentiation of somite lineages. *Mesp2* is a basic helix–loop–helix (bHLH) transcription factor required for normal rostral–caudal segmental polarity of somite tissue but not differentiation of somitic lineages, such as muscle (24). *LMO4* was expressed in presomitic mesoderm of *Mesp2* mutant embryos. However, activation of *LMO4* in the rostral portion of newly formed somites was not detectable (Fig. 4*G*). There-

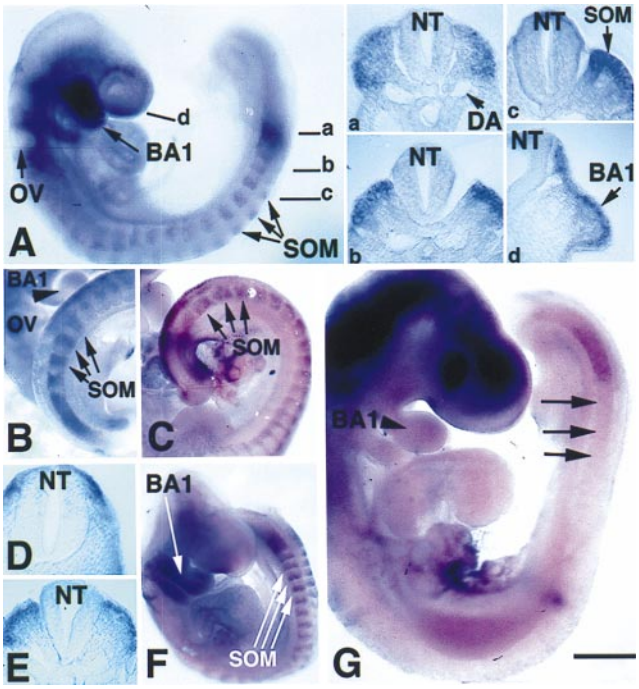

FIG. 4. Distribution of *LMO4* mRNA in cranial crest and paraxial mesoderm revealed by whole-mount *in situ* hybridization. (*A*) Sixteen somite-stage embryo exhibits *LMO4* expression (blue or brown stain) in cranial neural crest migrating into the branchial arches and in rostral somite. Sections at indicated axial levels show expression in dorsal paraxial mesoderm (a), prospective dermomyotome (b), dermomyotome (c), and migratory cranial neural crest in the mandibular component of the first branchial arch (BA1) (d). Otic vesicle (OV), neural tube (NT), and somites (SOM) are indicated by arrows. DA, dorsal aorta. (*B*) At E10, *LMO4* expression in paraxial mesoderm and in rostral somite halves persists at a caudal axial level (*E*) and is restricted medially at anterior levels to cells adjacent to the neural tube (*D*). (*B*) As indicated by arrowhead, *LMO4* expression was restricted to ventral mandibular arch by this stage. (*C*) *Pax3* expression is not restricted, but is distributed throughout the dermomyotome. (*F*) *LMO4* activation in *Splotch* mice is similar to normal embryos in migratory cranial neural crest cells and unsegmented paraxial mesoderm, yet somitic expression is not restricted medially. (*G*) In *Mesp2* mutant embryos, activation of *LMO4* in unsegmented mesoderm appears normal. However, expression is lost in rostral somite (arrow). Expression in mandibular arch is detected at a diminished level. Staining in the head region is an artifact caused by probe trapping. [Bar = 200 μm (*A*, *B*, *C*, and *G*) and 400 μm (*D* and *F*).]

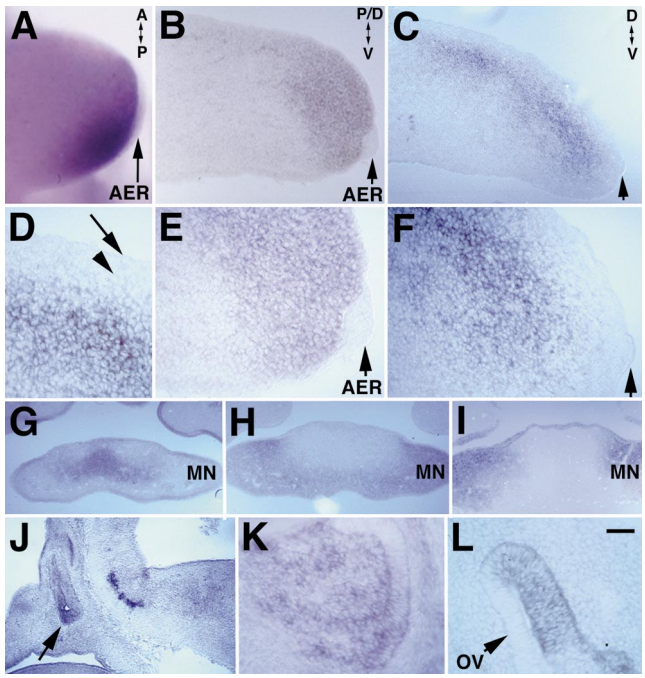

FIG. 5. Expression of *LMO4* and *LMO2* in limb tissue and expression of *LMO4* in ventral mandible, anterior pituitary, and otic vesicle revealed by nonisotopic *in situ* hybridization to tissue sections. (*A*, *B*, and *E*) *LMO2* is activated in posterior–distal mesenchyme subjacent to the AER (arrow) at E9.5 (*A*) and persists at E11.5 (*B* and *E*). *E* is a ×2.5 magnification of tissue in *B*. (*C*, *D*, and *F*) Activation of *LMO4* occurs in dorsal mesenchyme in E11.5 limb (*C*) that does not contact ectoderm (arrow) (*D* and *F*). Arrowhead marks subjacent mesenchyme. *D* and *F* are a ×2.5 magnification of *C*. Arrow in *C* and *F* indicate AER. (*G*) Near-adjacent sections show that activation of *LMO4* in E11.5 ventral mandible is restricted medially, while *Pax3* (*H*) and *Ptx1* (*I*) expression overlap in a complementary domain laterally. (*J* and *K*) Sagittal section through the head shows *LMO4* expression in anterior pituitary tissue at E11.5 (*J*) and E14.5 (*K*). Expression of *LMO4* persists in distinct regions of the otic vesicle (OV) at E11.5. [Bar = 60 μm (*A*), 50 μm (*B*, *C*, *G–J*), and 20 μm (*D–F*, *K*, *L*).]

fore, maintenance of *LMO4* expression in somite requires Mesp2 activity. Since *Mesp2* mutants have somitic derivatives such as muscle and sclerotome, we infer that *LMO4* is not required for differentiation of somitic lineages.

Expression of *LMO* Genes in Limb Bud and Mandibular Arch. During limb outgrowth and patterning, both *LMO2* and *LMO4* have expression domains that overlap with progress zone mesenchyme, with *LMO2* being expressed in distal and posterior mesenchyme (Fig. 5*A* and *B*), and *LMO4* in dorsal mesenchyme. At E11.5, *LMO4* expression was detected in dorsal mesenchyme extending along the proximal–distal axis of the limb bud (Fig. 5*C*). While *LMO4* transcripts were not detected in mesenchyme subjacent to overlying ectoderm (Fig. 5 *D* and *F*), *LMO2* transcripts were detected in mesenchyme subjacent to ectoderm and to the apical ectodermal ridge (AER) (Fig. 5*E*).

In the developing jaw, *LMO4* was expressed at high levels in both ventral and dorsal mandibular mesenchyme at E8.5 (Fig. 4*A*, d), yet between E9.5 and E11.5, expression was progressively restricted ventrally to the transitory mesenchyme that ultimately joins the left and right components of mandibular arch (Figs. 4*B* and 5*G*; data not shown). *Pax3* and *Ptx1* were coexpressed in a domain associated with differentiation of cartilage and muscle (25) that was complementary to the *LMO4* expression domain (Fig. 5 *G–I*). Therefore, *LMO4* expression was excluded from differentiating tissue and defined the transitory mesenchyme that joins the left and right mandibular arches at the midline.

LMO4 expression also was detected in nasalpharyngeal ectoderm and maxillary mesenchyme during mergence of the frontonasal process (Fig. 5*G*; data not shown). *LMO4* is activated in other tissues, including early motor neurons of the ocularmotor nerve, hindbrain motor neurons, glial cells associated with the optic nerve and cranial nerves, anterior pituitary, otic vesicle, and later in forebrain neurons (Fig. 5 *J–L*; data not shown). *LMO4* activation in the anterior pituitary first was detected at E11.5 and persisted until E14.5, the last time examined (Fig. 5 *J* and *K*). During ear development, expression of *LMO4* first appeared in the lateral wall of the closing otic vesicle and persisted in the semicircular canal primoridia at E11.5 (Fig. 5*L*).

***LMO4* Expression in Motor Neurons and Schwann Cell Progenitors.** At E11.5, the domain of *LMO4* expression extended more dorsally in rostral spinal cord relative to caudal levels (Fig. 6 *A* and *E*). Comparison of adjacent sections in the lumbar spinal cord shows that *LMO4* expression (Fig. 6 *B* and *F*) overlapped with *LHX3* expression in the medial subdivision of the median motor column (MMC_m), but not with *LHX3* expression in interneurons (Fig. 6 *C* and *G*). Expression of *LMO4* in cells slightly more dorsal to the MMC_m overlaps with

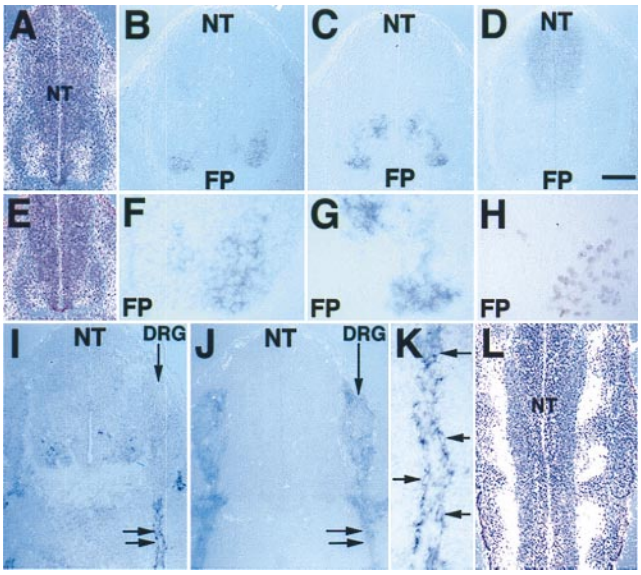

FIG. 6. Activation of *LMO4* in motor neurons and Schwann cell progenitors. (*A* and *E*) *In situ* hybridization of the ^{35}S-labeled *LMO4* probe to transverse sections counterstained with hematoxylin shows that the domain of *LMO4* neural tube (NT) expression (white grains) is broad at a rostral axial level (*A*) relative to caudal axial level (*E*). *In situ* hybridization of digoxygenin-labeled probes to adjacent transverse sections through the E11.5 lumbar spinal cord shows overlap of the *LMO4* expression pattern (Blue) (*B* and *F*) with motor neuron expression of *LHX3* (*C* and *G*), but not with *LHX3*-expressing interneurons. HRP immunohistochemistry shows that the expression domain of the pan-motor neuronal marker HB9 (*H*) on adjacent sections partially overlaps with *LMO4* and *LHX3* expression domains. FP, floor plate. *F* and *G* are ×2.5 magnifications of *B* and *C*, respectively. Apical paraventricular cells that express *LMO4* (*B*) do not overlap with the *Pax-3* expression domain (*D*). (*I*) At E11.5, activation of *LMO4* occurs in cells tightly associated with spinal nerves, indicated by double arrows. (*J*) *Sox10* expression in Schwann cells overlaps with *LMO4* expression (*I*). *K* is a ×3 magnification of the tissue in *I*. Arrows indicate individual cells decorating the spinal nerve that express *LMO4*. (*L*) Longitudinal section through the E11.5 neural tube hybridized with ^{35}S-labeled *LMO4* probe and counterstained with hematoxylin shows expression (white grains) at the exit points for spinal nerves. [Bar = 50 μm (*A–E*, *J*), 20 μm (*F–H*, *L*), 60 μm (*I*), and 12 μm (*K*).]

the pan-motor neuronal marker HB9 (Fig. 6*H*). Expression of *LMO4* in apically located paraventricular cells (Fig. 6*B*) does not overlap with the domain of *Pax3* expression (Fig. 6*D*). *LMO4* expression in motor neurons persisted at later times (data not shown). These data show that *LMO4* is activated in spinal cord motor neurons soon after neuroblast migration, during the period of neurite outgrowth.

LMO4 transcripts also were present in individual cells tightly associated with cranial and spinal nerves (Fig. 6 *I*, *K*, and *L*; data not shown). The glia marker *Sox10* (26) and *LMO4* have identical expression patterns along nerve fibers, but differ within the dorsal root ganglia (DRG), where *Sox10*, but not *LMO4*, is present at this stage (Fig. 6 *I* and *J*). Overlapping expression of *LMO4* and *Sox10* indicates that *LMO4* is activated in Schwann cell progenitors after their emergence from the DRG.

DISCUSSION

NLI:LIM Domain Complexes. LMO and LHX proteins form tetrameric complexes with NLI that are proposed to regulate gene expression (1). Because combinatorial association of LHX proteins is mediated by dimeric NLI (13), the widespread abundance of NLI provides for tetrameric regulatory complexes between LHX and LMO proteins. We show several cases in which LMO and LHX gene expression overlap. Although it is difficult to make a meaningful assessment of the biological relevance for NLI:LMO:LHX complexes, expression of *LMO4* and *LMO2* during early embryogenesis suggests a possible role in maintenance of an undifferentiated state, potentially by disruption of LHX activity.

LMO4 expression in dorsal limb mesenchyme partially overlaps with the LHX gene *Lmx1*, which is thought to dorsalize the limb in response to Wnt7a (for review, see ref. 27). The time and location of *LMO4* activation implicate *LMO4* as a possible gene target of Lmx1. *NLI* is widely expressed in E10.5 limb mesenchyme and, like *LMO4* and *LMO2*, is restricted to perichondral tissue during digit formation at E14.5 (data not shown). Since synergistic interactions between Lmx1 and E47 are disrupted by NLI (28), formation of complexes containing NLI and Lmx1 in subectodermal limb mesenchyme are likely to modulate Lmx1 activity during limb dorsalization. In deeper mesenchyme, LMO4 likely would modify the NLI:Lmx1 complex. Identification of *LMO4* as both a potential gene target and transcriptional modulator of Lmx1 activity should help define the role of Lmx1 during limb patterning.

In the spinal cord, motor neurons are parsed into an array of functionally distinct motor columns, with each column defined by combinatorial expression patterns of LHX genes (29). We show that the spinal cord is further imbricated by expression of *LMO4*. The activation of *LMO4* in E10.5 motor neurons occurs after the onset of high levels of Isl1 and NLI expression at E9.5 (10). Therefore, LMO4 likely modulates the transcriptional activity of NLI:Isl1 complexes after the initial role of Isl1 in the generation of motor neurons.

LMO Expression in Uncommitted Tissue. The activation of *LMO2* adjacent to the zone of polarizing activity (ZPA) and subjacent to the AER defines a unique population of mesenchyme that connects the AER and ZPA signaling centers of the limb. The lack of commitment within the progress zone that underlies the AER is linked to continued outgrowth of the limb, and both qualities are stimulated by reciprocal interactions of the ZPA with the AER (27). A potential role for LMO2 in blocking commitment of progress zone-associated tissue to regional fates conforms with the functional precedent for LMO2 in inhibition of cellular differentiation (30, 31).

Schwann cell progenitors activate *LMO4* after making axonal contact, during the period in which Schwann cell differentiation is delayed (32). Schwann cell progenitors within the DRG remain multipotent, capable of forming both Schwann and pigment cells (33). Expression of *LMO4* first is detected after Schwann cell progenitors emerge from DRG and contact spinal nerves, raising the possibility that axonal contact activates *LMO4*.

LMO4 and *LMO2* are regulated differentially during the development of thymic subsets. A role for LMO2 in promotion of blast proliferation and inhibition of T lymphocyte differentiation was proposed based on analysis of transgenic animals (31). Our data showing blast cell expression of *LMO2* suggest a role for *LMO2* in normal T cell proliferation. The demonstration that ectopic expression of either *LMO1* or *LMO2* leads to tumorigenesis in T cells (6, 21) suggests that these structurally related proteins perform a similar function in cell growth. The normal expression of *LMO4* in all thymic subsets and coexpression of *LMO2* and *LMO4* in proliferating blast cells suggest that T cell proliferation or differentiation may be determined by the level of LMO expression.

LMO4 activation by migratory cranial neural crest cells and transitory mesenchyme defines a stage when these tissues are uncommitted to regional fates. Cranial neural crest cells are generated at the boundary between ectoderm and neural epithelia (34), yet are prevented from becoming either ectoderm or neural epithelial derivatives. Activation of *LMO4* expression at the onset of migration marks the time of divergence between the cranial neural crest cell lineage and the

ectodermal and neural tube cell lineages. *LMO4* expression similarly distinguishes transitory mesenchyme, which establishes continuity between the core mesenchymal components of each mandibular process, from neighboring differentiating mesenchyme. Therefore, *LMO4* expression in the mandibular arch characterizes uncommitted tissue that supports morphological transformations essential for facial development.

Regulation of LMO4. Lack of *LMO4* expression in *Mesp2* mutant embryos demonstrates that *LMO4* activation is regulated during the establishment of somite formation and that somites in *Mesp2* mutants lack a rostral character. Although the significance of rostral–caudal differences in the dermomyotome is unclear, the rostral–caudal differences in newly formed somites are likely to mediate the formation of somite boundaries. Maintenance of both *LMO4*- and *Notch*-signaling molecules during somite development requires *Mesp2*, but it remains to be determined whether *Notch* signaling and *LMO4* act together or in parallel. Alternatively, *LMO4* activation could be downstream of FGFR1 activation, since FGFR1 somitic expression also is absent in *Mesp2* mutant mice (24).

The diversity seen in expression of LMO4 may be indicative of a fundamental mechanism of gene regulation that is common to separate patterning events. In addition to LMO4, signaling mechanisms that involve BMPs, fibroblast growth factors, sonic hedgehog, and wingless proteins are reiterated during patterning of the face, limb, and somite (27, 36–38). Therefore, via interaction with NLI, LMO4 may modulate the activity of transcriptional complexes in response to highly conserved signaling mechanisms that pattern the early embryo.

We are grateful to the following people for helpful discussions and assistance: David Schwarz for assistance with isolation of thymic sublineages, Sam Pfaff for the HB9 antibody, and Martyn Goulding for the *Splotch* mice and Pax3 cDNA. We thank Heiner Westphal for the Lhx3 cDNA, Michael Wegner for the Sox10 cDNA, and Jacque Drouin and Pamela Mellon for the Ptx1 cDNA. These studies were supported by National Institutes of Health Grant DK13149. D.A.K. is supported by National Institutes of Health Training Grant T32HL07770 and L.W.J. is supported by National Institutes of Health Training Grant DK07541.

1. Dawid, I. B., Breen, J. J. & Toyama, R. (1998) *Trends Genet.* **14,** 156–162.
2. Shawlot, W. & Behringer, R. R. (1995) *Nature (London)* **374,** 425–430.
3. Pfaff, S. L., Mendelsohn, M., Stewart, C. L., Edlund, T. & Jessell, T. M. (1996) *Cell* **84,** 309–320.
4. Boehm, T., Foroni, L., Kaneko, Y., Perutz, M. F. & Rabbitts, T. H. (1991) *Proc. Natl. Acad. Sci. USA* **88,** 4367–4371.
5. Royer-Pokora, B., Loos, U. & Ludwig, W.-D. (1991) *Oncogene* **6,** 1887–1893.
6. Fisch, P., Boehm, T., Lavenir, I., Larson, T., Arno, J., Forster, A. & Rabbitts, T. H. (1992) *Oncogene* **7,** 2389–2397.
7. Warren, A. J., Colledge, W. H., Carlton, M. B., Evans, M. J., Smith, A. J. & Rabbits, T. H. (1994) *Cell* **78,** 45–57.
8. Yamada, Y., Warren, A. J., Dobson, C., Forster, A., Pannell, R. & Rabbitts, T. H. (1998) *Proc. Natl. Acad. Sci. USA* **95,** 3890–3895.
9. Wadman, I. A., Osada, H., Grutz, G. G., Agulnick, A. D., Westphal, H., Forster, A. & Rabbitts, T. H. (1997) *EMBO J.* **16,** 3145–3157.
10. Jurata, L. W., Kenny, D. A. & Gill, G. N. (1996) *Proc. Natl. Acad. Sci. USA* **93,** 11693–11698.
11. Agulnick, A. D., Taira, M., Breen, J. J., Tanaka, T., Dawid, I. B. & Westphal, H. (1996) *Nature (London)* **384,** 270–272.
12. Bach, I., Carriere, C., Ostendorff, H. P., Andersen, B. & Rosenfeld, M. G. (1997) *Genes Dev.* **11,** 1370–1380.
13. Jurata, L. W., Pfaff, S. L. & Gill, G. N. (1998) *J. Biol. Chem.* **273,** 3152–3157.
14. Morcillo, P., Rosen, C., Baylies, M. K. & Dorsett, D. (1997) *Genes Dev.* **11,** 2729–2740.
15. Schaeren-Wiemers, N. & Gerfin-Moser, A. (1993) *Histology* **100,** 431–440.
16. Angerer, L. M., Toler, M. H. & Angerer, R. C. (1987) in *In Situ Hybridization–Applications to Neurobiology,* eds. Valentino, K. L., Eberwine, J. H. & Barchas, J. D. (Oxford Univ. Press, Oxford), pp. 42–70.
17. Wilkinson, D. G. & Nieto, M. A. (1993) *Methods Enzymol.* **225,** 361–373.
18. Foroni, L., Boehm, T., White, L., Forster, A., Sherrington, P., Liao, X. B., Brannan, C. I., Jenkins, N. A., Copeland, N. G. & Rabbitts, T. H. (1992) *J. Mol. Biol.* **226,** 747–761.
19. Zhu, T. H., Bodem, J., Keppel, E., Paro, R. & Royer-Pokora, B. (1995) *Oncogene* **11,** 1283–1290.
20. Neale, G. A. M., Mao, S., Parham, D. M., Murti, K. G. & Goorha, R. M. (1995) *Cell Growth Differ.* **6,** 587–596.
21. McGuire, E. A., Rintoul, C. E., Sclar, G. M. & Korsmeyer, S. J. (1992) *Mol. Cell. Biol.* **12,** 4186–4196.
22. Goulding, M., Sterrer, S., Fleming, J., Balling, R., Nadeau, J., Moore, K. J., Brown, S. D. J., Steel, K. P. & Gruss, P. (1993) *Genomics* **17,** 355–363.
23. Goulding, M., Lumsden, A. & Paquette, A. J. (1994) *Development* **120,** 957–971.
24. Saga, Y., Hata, N., Koseki, H. & Taketo, M. M. (1997) *Genes Dev.* **11,** 1827–1839.
25. Lanctot, C., Lamolet, B. & Drouin, J. (1997) *Development* **124,** 2807–2817.
26. Kuhlbrodt, K., Herbarth, B., Sock, E., Hermans-Borgmeyer, I. & Wenger, M. (1998) *J. Neurosci.* **18,** 237–250.
27. Johnson, R. L. & Tabin, C. J. (1997) *Cell* **90,** 979–990.
28. Jurata, L. W. & Gill, G. (1997) *Mol. Cell. Biol.* **17,** 5688–5698.
29. Tsuchida, T., Ensini, M., Morton, S. B., Baldassare, M., Edlund, T., Jessell, T. M. & Pfaff, S. L. (1994) *Cell* **79,** 957–970.
30. Visvader, J. E., Mao, X., Fujiwara, Y., Kyungmin, H. & Orkin, S. H. (1997) *Proc. Natl. Acad. Sci. USA* **94,** 13707–13712.
31. Neale, G. A. M., Rehg, J. E. & Goorha, R. M. (1995) *Blood* **86,** 3060–3071.
32. Monuki, E. S., Weinmaster, G., Kuhn, R. & Lemke, G. (1989) *Neuron* **3,** 783–793.
33. Stocker, K. M., Sherman, L., Rees, S. & Ciment, G. (1991) *Development* **111,** 635–645.
34. Selleck, M. A. & Bronner-Fraser, M. (1995) *Development* **121,** 525–538.
35. Zhang, H., Hu, G., Wang, H., Sciavolino, P., Iler, N., Shen, M. M. & Abate-Shen, C. (1997) *Mol. Cell Biol.* **17,** 2920–2932.
36. Hogan, B. L. M. (1996) *Genes Dev.* **10,** 1580–1594.
37. Wall, N. A. & Hogan, B. L. M. (1995) *Mech. Dev.* **53,** 383–392.
38. Richman, J. M. & Tickle, C. (1992) *Dev. Biol.* **154,** 299–308.